Carbon Nanotubes

DOI: 10.1002/anie.201204791

Statistical Raman Spectroscopy: An Method for the Characterization of Covalently Functionalized Single-Walled Carbon Nanotubes**

*Ferdinand Hof, Sebastian Bosch, Jan M. Englert, Frank Hauke, and Andreas Hirsch**

Covalent chemical functionalization of single-walled carbon nanotubes (SWCNTs) has become a very important subject within the field of carbon allotrope research.[1] It allows a number of intrinsic hurdles to be overcome, such as aggregation, low solubility, and difficult processability, which impede a straightforward development of SWCNTs as building blocks in high-performance materials. Chemical functionalization offers the opportunity to combine their unprecedented properties with those of other compound classes and it is a promising approach for separation by electronic properties. A number of reactions have been reported that show preferential attack of addends to either metallic or semiconducting tubes.[2] We have recently demonstrated a selective carboxylation of semiconducting tubes that were exfoliated and reduced under modified Birch conditions.[3] Nevertheless, an efficient large-scale separation of metallic tubes from semiconducting tubes is still a major challenge in carbon nanotube chemistry. Therefore, analytical methods that provide reliable and direct insights into the degree of covalent functionalization, homogeneity of the bulk sample, and overall selectivity by electronic properties are particularly desirable. Although conventional Raman spectroscopy provides important information with respect to covalent modifications of SWCNTs, it lacks a quantitative description about the distribution of properties in the bulk material. It has turned out that Raman spectra recorded at different spots may vary considerably (Supporting Information, Figure S1). This leads to severe misinterpretations on the specific outcome of a reaction. As a consequence, comparability between different reaction products is not provided. Herein, we present the use of scanning Raman microscopy (SRM) and the corresponding statistical data analysis for the unequivocal characterization of covalently functionalized SWCNTs. With the introduction of the Raman defect (RDI), Raman homogeneity (RHI), and Raman selectivity indices (RSI), we are now able to provide a straightforward and unambiguous direct insight into the degree of functionalization as well as into the product homogeneity and the selectivity of a reaction sequence. We present this quantification upon analyzing a number of differently functionalized reaction products (Scheme 1).

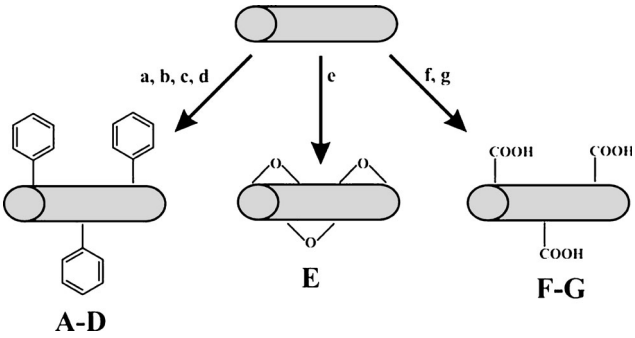

Scheme 1. Model systems for statistical Raman analysis. Reaction of SWCNTs with benzenediazonium tetrafluoroborate (BDT)[2a] after different proceeding activation steps: a) after modified Birch reduction, b) after 20 min of ultrasonication of neutral SWCNTs in cyclohexyl pyrrolidone (CHP) followed by addition of BDT, c) after 20 min of ultrasonication of neutral SWCNTs in THF followed by addition of BDT, d) after reaction of SWCNTs with BDT during 10 min of ultrasonication. e) Epoxidation of SWCNTs[7] with *m*-CPBA after 20 min of ultrasonication in CHP. f, g) Carboxylation of SWCNTs with CO_2 after different activation steps: f) after modified Birch reduction,[3] g) after reduction in a Na/K alloy and 20 min of ultrasonication in THF.

We initially focus on the data analysis of the reaction product of a new functionalization sequence, namely the wet chemical treatment of negatively charged tubes with benzenediazonium tetrafluoroborate (BDT; Scheme 1a, Figure 1a). Later on these results are compared with those obtained for other covalent derivatization sequences. The corresponding SWCNT reduction has been carried out under our previously reported modified Birch conditions[4] with lithium metal in liquid ammonia and THF as a co-solvent. After evaporation of the ammonia, the diazonium salt was carefully added to the negatively charged nanotubes, followed by an aqueous work-up of the reaction product. In contrast to the reaction of neutral SWCNTs with diazonium salts, originally introduced by Tour et al.,[5] we expect that the Coulomb attraction between the negatively charged tubes and the positively charged diazonium species will further increase the efficiency of the addition reaction.

The reaction product **A** was characterized by TG/MS analysis (Supporting Information, Figure S2) and by statistical Raman analysis. For this purpose, mappings of 10000 μm^2, which corresponds to 2500 spectra in each, were carried out (Figure 1b). In general the D-band intensity is a measure for

[*] F. Hof, S. Bosch, J. M. Englert, F. Hauke, Prof. Dr. A. Hirsch
Department of Chemistry and Pharmacy and Institute of Advanced Materials and Processes (ZMP), University of Erlangen-Nuremberg
Henkestrasse 42, 91054 Erlangen (Germany)
E-mail: andreas.hirsch@chemie.uni-erlangen.de
Homepage: http://www.zmp.uni-erlangen.de

[**] The authors thank the Deutsche Forschungsgemeinschaft (DFG-SFB 953, Project A1 "Synthetic Carbon Allotropes"), the Interdisciplinary Center for Molecular Materials (ICMM), the European Research Council (ERC; grant 246622 GRAPHENOCHEM), and the Graduate School Molecular Science (GSMS) for financial support.

Supporting information for this article is available on the WWW under http://dx.doi.org/10.1002/anie.201204791.

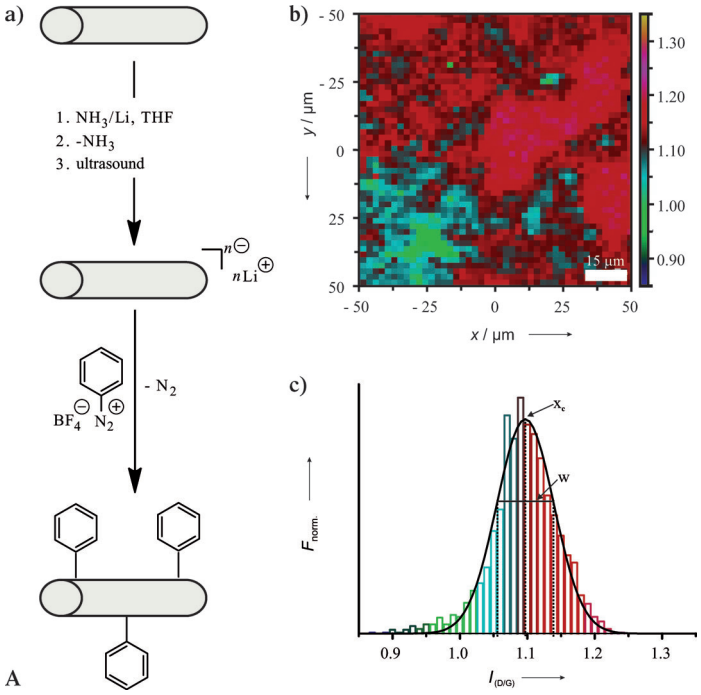

Figure 1. a) Arylation of SWCNTs by reduction and subsequent reaction with diazonium salts yielding product **A**. b) Scanning Raman map: 10000 µm², 2500 spectra, excitation wavelength 532 nm (the different colors encode the spatially resolved $I_{(D/G)}$ values; that is, the ratio of the intensities of the D- and G-band maxima); c) Histogram of the $I_{(D/G)}$ values. The black curve represents the corresponding Gaussian root-mean-square fit; the different colors represent the respective spatially resolved $I_{(D/G)}$ values in the Raman map. The maximum (x_c) is a measure of the mean degree of functionalization and the width (w) correlates with the sample homogeneity.

the amount of sp^3 defects introduced by covalent addend binding.[6] Therefore, the $I_{(D/G)}$ ratio of every point spectrum was determined and subsequently their frequency was grouped into a histogram (Figure 1c), which follows a Gaussian distribution characterized by the maximum x_c and the width w of $\pm\sigma$, where $\pm\sigma$ is the standard deviation of the data set and is a measure for the homogeneity of the D-band active defects.

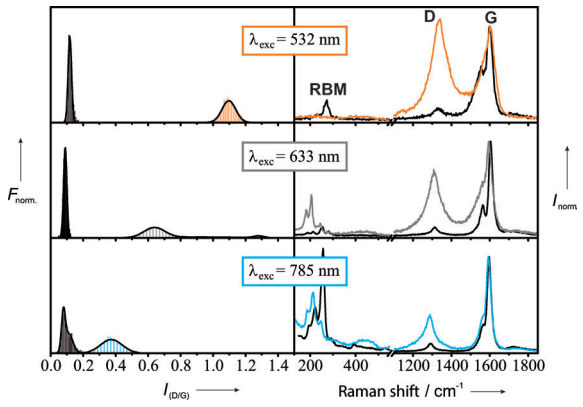

Figure 2. Raman analysis of the reaction product **A** at three different excitation wavelengths: Left: $I_{(D/G)}$ histograms of the pristine material (black) and of the functionalized sample **A**; right: median spectra of the corresponding histograms. RBM = radial breathing modes.

By comparison of the data obtained for three laser excitation wavelengths (532, 633, and 785 nm), an even more comprehensive picture of the reaction outcome is captured (Figure 2), as the electronic selectivity can also be analyzed. In the case of **A**, the value determined for x_c at 532 nm, where predominantly metallic tubes are in resonance, is much larger than the value determined at 785 nm, where mainly semiconducting species are probed. An intermediate situation is observed for an excitation at 633 nm, where both species are excited simultaneously. Obviously, the example reaction depicted in Figure 1a shows selectivity towards a preferential functionalization of metallic SWCNTs.

For the quantification of the reaction outcome, we introduce the indices RDI, RHI, and RSI. The Raman defect index (RDI) can be obtained directly from the respective Gaussian distributions by plotting the frequency of $I^{532}_{(D/G)}$ versus $I^{785}_{(D/G)}$ (Figure 3). It is defined [Eq. (1)] as the length of the vector spanning the origin

$$\mathrm{RDI}_{(A)} = |\vec{a}| = \sqrt{\left(x_c^{532}\right)^2 + \left(x_c^{785}\right)^2} \quad (1)$$

and (x_c^{532}, x_c^{785}). For the reaction product **A** (Figure 1a), the corresponding $\mathrm{RDI}_{(A)}$ value is 1.15, while the RDI of the starting material **P** ($\mathrm{RDI}_{(P)}$) is as low as 0.15.

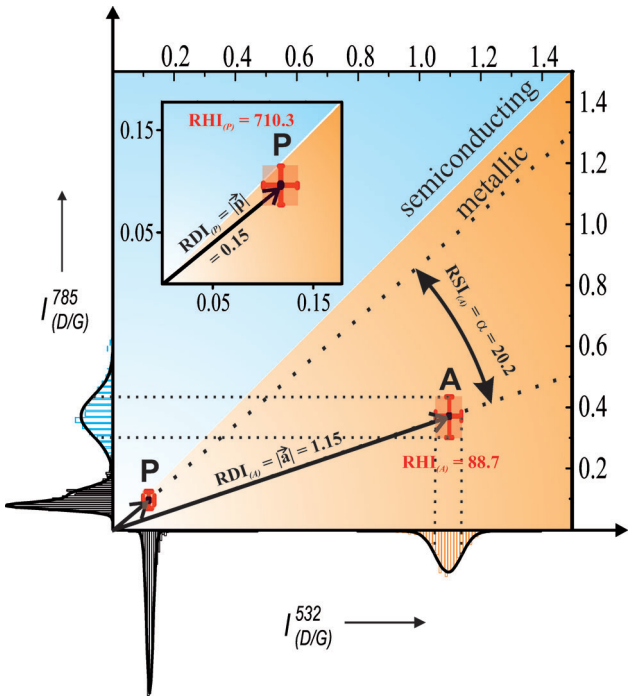

Figure 3. 2D representation of a statistical Raman analysis comparing the starting material **P** with the reaction product **A** at λ_{exc} of 532 nm (metallic) and 785 nm (semiconducting). The accounts of the vectors correspond to the Raman defect index (RDI) at the corresponding excitation wavelengths. The red crosses indicate the standard deviations whose reciprocal products determining the Raman homogeneity indices (RHI) are illustrated by the red-shaded rectangles. The angle α describes the Raman selectivity index (RSI). Electronic-type preferences can be found in the orange (metallic) and in the blue-shaded (semiconducting) regions.

The second characteristic parameter RHI, which is a measure for the sample polydispersity, can be obtained from the respective standard deviations. It is defined as reciprocal product of w^{532} and w^{785} [Eq. (2)]. The superscripts

$$\mathrm{RHI}_{(A)} = (w^{532} \times w^{785})^{-1} \quad (2)$$

532 and 785 denote the wavelengths where either metallic SWCNTs or semiconducting tubes are in resonance. As can be seen in Figure 3, the pristine starting material with a $\mathrm{RHI}_{(P)} = 710.3$ is a more homogeneous material with respect to defect density in comparison to the reaction product **A** with $\mathrm{RHI}_{(A)} = 88.7$. This clearly reflects a decrease of sample homogeneity after the functionalization.

The Raman-selectivity index (RSI) is defined as the angle between the vectors of the pristine material and the functionalized sample. In the case of an electronic-type selective functionalization, the corresponding RDI vector is allocated in either the metallic or the semiconducting region. The magnitude of the RSI is a measure for the grade of the electronic-type selectivity. In the case of reaction **A** (Figure 1 a), the $\mathrm{RSI}_{(A)}$ vector is allocated in the metallic regime with a value of 20.2°.

$$\mathrm{RSI}_{(A)} = a = \arccos\left(\frac{\vec{p}\vec{a}}{|\vec{p}||\vec{a}|}\right) \quad (3)$$

The outcome of addition reactions to carbon nanotubes can now easily be analyzed by the determination of the Raman indices. This will be demonstrated by a comparison of the products **B**–**G** (Figure 4, Table 1) obtained from the reactions sequences depicted in Scheme 1 (for corresponding Raman data see the Supporting Information, Figures S3–S8).

The reaction of SWCNTs with diazonium compounds can be carried out as solvent-free functionalizations[8] in aqueous[4b] and organic[9] media. Here, selectivity towards metallic SWCNTs was observed with surfactant-wrapped nanotubes in water.[2a] Taking into account that nanotube individualization is necessary for selective reactions, we used different activation processes to generate debundled SWCNTs. As it turned out, the RDI values for the products **B**, **C**, and **D** (Scheme 1, Table 1) obtained after the reaction of neutral nanotubes with BDT are considerably lower compared to the sequences based on charged SWCNT intermediates. They also differ significantly depending on the dispersion conditions. It is reasonable to assume that a high grade of debundling is required for an efficient and homogenous functionalization. It has been observed that especially cyclohexyl pyrrolidone (CHP) is capable to individualize SWCNTs,[10] which in turn leads to higher RDIs as corroborated by this study (Table 1). Debundling is also facilitated by ultrasonication (Scheme 1, **D**) and leads to increased RDI values. For all three examples, this is accompanied by an increase of RSI (Table 1). We thus conclude that both the degree of functionalization and the selectivity of a comparable reaction sequence depends significantly on the degree of debundling.[3]

For the majority of covalent SWCNT functionalization sequences, no electronic-type preferences have been reported. With the aid of the analysis presented herein, we

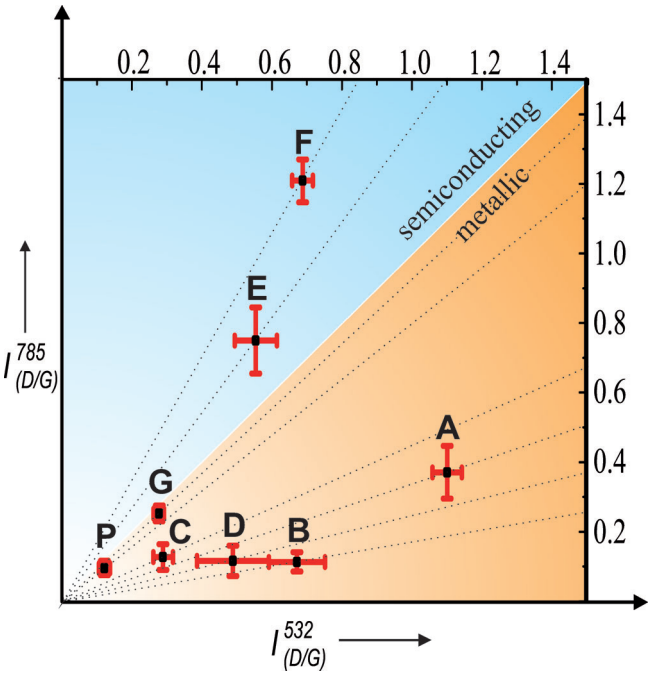

Figure 4. 2D plot of the statistical Raman analysis comparing the starting material **P** to the reaction products **A**–**G** depicted in Scheme 1. For the values of RDI, RSI, and RHI, see Table 1.

Table 1: Raman indices of reaction products **A**–**G**.

	F	B	C	D	E	F	G
RDI	1.15	0.67	0.31	0.50	0.93	1.39	0.37
RSI	20.2	29.2	14.7	25.3	14.9	21.7	3.9
RHI	88.7	198.1	330.1	64.1	45.0	171.1	1113.4

can easily sense even subtle electronic-type preferences, indicated by the respective RSI values (Table 1, Figure 4). For example, in addition to the previously reported epoxidation of SWCNTs with 3-chloroperoxybenzoic acid (*m*-CPBA) in CH_2Cl_2,[7] we found for **E** a slight selectivity towards semiconducting nanotubes in CHP. No electronic-type preference and a low degree of functionalization were found for the carboxylation of SWCNTs reduced with a Na/K alloy (Scheme 1, **G**). In contrast, the functionalization with CO_2 under modified Birch conditions (Scheme 1, **F**) yields the highest degree of functionalization, with selectivity towards semiconducting SWCNTs (Table 1, Figure 4). This confirmed our expectations on the basis of our fundamental investigation on the carboxylation of SWCNTs,[3] where we indicated that an efficient debundling has a pronounced effect on the outcome of the reaction. Another significant result that was derived is that a higher degree of functionalization is in general accompanied by a lower homogeneity of the reaction product as expressed by an decreased RHI value.

In conclusion, we have introduced an efficient concept for the classification of covalent addition reactions to SWCNTs in terms of degree of functionalization, electronic-type selectivity, and sample homogeneity. This method, which is based on statistical Raman analysis, will be useful for the systematic

development of novel functionalization concepts for the efficient bulk isolation of either metallic or semiconducting SWCNT species, for example. This will in turn be the foundation for the application of carbon nanotubes in future electronic devices. Furthermore, this study is a considerable step forward in gaining clear insights into fundamental chemical properties of carbon nanotubes.

Experimental Section

Raman spectroscopic characterization was carried out on a Horiba LabRAM Aramis confocal Raman microscope (λ_{exc}: 532, 633, and 785 nm) with a laser spot size of about 1 μm (Olympus LMPlanFl 100 μ, NA 0.80). The incident laser power was kept as low as possible to avoid structural sample damage: 240 μW (532 nm), 114 μW (622 nm), and 3 mW (785 nm). Spectra were obtained by a CCD array at −70 °C and a 600 grooves/mm (523 & 633 nm) or 300 grooves/mm grating from a 100 μm × 100 μm area with 2 μm step size in SWIFT mode for low integration times. Sample movement was obtained by an automated XY-scanning table. Further experimental details can be found in the Supporting Information.

Received: June 19, 2012
Published online: October 25, 2012

Keywords: carbon allotropes · functionalization · nanotubes · Raman spectroscopy · statistical methods

[1] a) A. Hirsch, *Angew. Chem.* **2002**, *114*, 1933; *Angew. Chem. Int. Ed.* **2002**, *41*, 1853; b) Z. Chen, W. Thiel, A. Hirsch, *ChemPhysChem* **2003**, *4*, 93; c) J. L. Bahr, J. M. Tour, *J. Mater. Chem.* **2002**, *12*, 1952; d) C. A. Dyke, J. M. Tour, *J. Phys. Chem. A* **2004**, *108*, 11151.

[2] a) M. S. Strano, C. A. Dyke, M. L. Usrey, P. W. Barone, M. J. Allen, H. Shan, C. Kittrell, R. H. Hauge, J. M. Tour, R. E. Smalley, *Science* **2003**, *301*, 1519; b) R. Graupner, J. Abraham, D. Wunderlich, A. Vencelová, P. Lauffer, J. Röhrl, M. Hundhausen, L. Ley, A. Hirsch, *J. Am. Chem. Soc.* **2006**, *128*, 6683; c) C. D. Doyle, J.-D. R. Rocha, R. B. Weisman, J. M. Tour, *J. Am. Chem. Soc.* **2008**, *130*, 6795; d) W.-J. Kim, N. Nair, C. Y. Lee, M. S. Strano, *J. Phys. Chem. C* **2008**, *112*, 7326; e) G. Schmidt, A. Filoramo, V. Derycke, J.-P. Bourgoin, P. Chenevier, *Chem. Eur. J.* **2011**, *17*, 1415.

[3] B. Gebhardt, F. Hof, C. Backes, M. Müller, T. Plocke, J. Maultzsch, C. Thomsen, F. Hauke, A. Hirsch, *J. Am. Chem. Soc.* **2011**, *133*, 19459.

[4] a) J. L. Bahr, J. Yang, D. V. Kosynkin, M. J. Bronikowski, R. E. Smalley, J. M. Tour, *J. Am. Chem. Soc.* **2001**, *123*, 6536; b) C. A. Dyke, J. M. Tour, *Nano Lett.* **2003**, *3*, 1215.

[5] B. Gebhardt, Z. Syrgiannis, C. Backes, R. Graupner, F. Hauke, A. Hirsch, *J. Am. Chem. Soc.* **2011**, *133*, 7985.

[6] L. G. Cançado, A. Jorio, E. H. M. Ferreira, F. Stavale, C. A. Achete, R. B. Capaz, M. V. O. Moutinho, A. Lombardo, T. S. Kulmala, A. C. Ferrari, *Nano Lett.* **2011**, *11*, 3190.

[7] D. Ogrin, J. Chattopadhyay, A. K. Sadana, W. E. Billups, A. R. Barron, *J. Am. Chem. Soc.* **2006**, *128*, 11322.

[8] C. A. Dyke, J. M. Tour, *J. Am. Chem. Soc.* **2003**, *125*, 1156.

[9] J. L. Bahr, J. M. Tour, *Chem. Mater.* **2001**, *13*, 3823.

[10] S. D. Bergin, Z. Sun, P. Streich, J. Hamilton, J. N. Coleman, *J. Phys. Chem. C* **2009**, *114*, 231.

